Hydrophobic Microcrystalline Cellulose/ Polyethyleneimine Composite Aerogel for Effective Sound Absorption

Xin Jia,[a,b] Guijiang Tang,[a,b] Jinming Gao,[a,b] Yangmiao Liao,[a,b] Yu Zhang,[a,b] Xueliang Jiang,[a,b] Huan Yang,[a,b] Dan Wu,[a,b] Feng You,[a,b] Peng Yu,[a,b] and Chu Yao [a,b,*]

A hydrophobic and ultralight cellulose aerogel (CA) was reinforced by polyethyleneimine (PEI) and functionalized by methyltrimethoxysilane (MTMS). Adding PEI improved the mechanical strength and the elastic resilience of the resulting material due to the flexibility enhancement of the cellulose chains, which prevented the collapse of the pore structure and contributed to the uniform pore size distribution. The hydrophobic property of the aerogels with the functionalization of MTMS was improved, which can prevent the pore structure from collapsing due to the absorption of water. The maximum compression modulus of aerogel reached 1.1 MPa at the strain of 80%, and its hydrophobic water contact angle was up to 112°. The hydrophobic composite aerogels exhibited ultrahigh efficiency in sound absorption across a wide frequency range from 500 to 6300 Hz, and their average absorption coefficient was greater than 0.74. The light weight, high porosity, and environmentally friendly aerogels presented in this work are promising for efficient sound absorption. They have potential applications in noise pollution treatment.

DOI: 10.15376/biores.18.4.8432-8443

Keywords: Cellulose; Aerogel; Compressive properties; Hydrophobic modification; Sound absorption; Polyethyleneimine

*Contact information: a: Hubei Key Laboratory of Plasma Chemistry and Advanced Materials, China; b: College of Materials Science and Engineering, Wuhan Institute of Technology, Wuhan 430205, China; * Corresponding author: chuyao@wit.edu.cn (C.Y.)*

INTRODUCTION

As a major social problem, noise pollution threatens human physical and mental health (Park *et al*. 2020; Moroe and Mabaso 2022). Therefore, developing advanced sound-absorbing materials is crucial. Porous material presents excellent acoustic properties in the wide frequency range (Cheng *et al*. 2016; Ren *at al*. 2022). Porous materials allow more sound waves to enter into the matrix during the propagation process (Arenas and Crocker 2010). Furthermore, the vibrational friction of the air in the porous structure is beneficial to dissipating the sound energy *via* heat losses and viscous losses. As a result, porous materials work well over a wide frequency band.

Commercial porous acoustic materials are mostly inorganic materials or synthetic polymer materials, including rock wool, glass wool, polyurethane, and other petroleum-based polymer materials (Bagheri *at al*. 2022; Wang *at al*. 2022; Salino and Catai 2023). These materials mostly have high costs and are difficult to degrade, resulting in irreversible effects on the environment.

Recently, biomass degradable natural materials have found applications in

acoustics (Pedroso *et al*. 2017). Some agricultural by-products (Lim *et al*. 2018; Samaei *at al*. 2023), such as coconut fiber, natural red hemp fiber, oil palm empty fruit bundle fiber, corn peel, and other organic natural fiber materials are readily available. More importantly, their average absorption coefficients at 500 to 6000 Hz can reach more than 0.5 to 0.6. Thus, the natural materials match some commercial synthetic materials in sound absorption performance. However, natural fiber materials have the disadvantages of poor mechanical properties, easy degradation by microorganisms, excessive density volume, and easy moisture absorption, which affects the acoustic performance of the materials.

As an important natural fiber materials, cellulosic materials with the merits of biodegradability, sustainability, and ease of modification (Soatthiyanon *et al*. 2020; Bian *et al*. 2021), have received much attention in the development of biomedicine (Li *et al*. 2015; Duan *at al*. 2023), oil/chemical spill treatment (Zhou *et al*. 2020), thermal insulation, and flame retardant materials (Yang *et al*. 2012; Guo *et al*. 2018). Moreover, cellulose can be used to prepare nascent third-generation aerogels which are considered as efficient porous sound absorption materials. The cellulose aerogels (CA) possess excellent properties with high porosity, high specific surface area, low photorefractive index, and low dielectric constant compared to traditional aerogels. The method of preparing cellulose aerogels consists of three main steps including dissolution, regeneration, and drying (Wang *et al*. 2012). Some intermediate treatment (*e.g.*, freeze-thawing or pre-gelation) is usually carried out after the cellulose has been dissolved (Lu *et al*. 2012; Wan *et al*. 2016) for certain purposes such as increasing the entanglement of cellulose molecules. Among these, the establishment of aerogel skeleton and the control of pore structure via physical cross-linking (Zhang *et al*. 2018) or chemical cross-linking (Guo *et al*. 2018) during pre-gelation of cellulose solutions are pivotal to carry out the application in various areas. Most research on cellulose aerogels has focused on the application of oil absorption (Rafieian *et al*. 2018), but no systematic report has been found in the acoustics field. According to acoustics theory, the high porosity and the suitable pore structure of cellulose aerogels can increase the dissipation of sound inside the material (Cao *et al*. 2018). The good compression recovery can satisfy the application requirement of sound absorption materials, and the necessary hydrophobic modifications can prevent the pore structure inside the cellulose aerogels from collapsing due to the absorption of water.

In this study, a composite cellulose aerogel (CA) with excellent mechanical properties, hydrophobicity, and ultrahigh efficiency in sound absorption was constructed by adopting microcrystalline cellulose (MCC) as host material, epichlorohydrin (EC) as crosslinker and polyethyleneimine (PEI) as reinforcing agent, and methyltrimethoxysilane (MTMS) as hydrophobic agent.

EXPERIMENTAL

Materials

Microcrystalline cellulose (MCC, its number average molecular weight is about 28400) was provided by the Sinopharm Group Chemical Reagent Co. Sodium hydroxide and urea were provided by Xi Long Chemical Co. Epichlorohydrin was purchased from the Sinopharm Group Chemical Reagent Co; polyethyleneimine (PEI) was purchased from the Nanjing Chemical Reagent Co. Methyltrimethoxysilane was provided by the Hubei Nan Xing Chemical General Factory. Deionized water in this experiment was self-made. All chemicals were used as received.

Preparation of Cellulose/Polyethyleneimine Composite Aerogel

The microcrystalline cellulose was pretreated by rinsing repeatedly with deionized water and anhydrous ethanol. After drying, 4 g of cellulose was added into a sodium hydroxide/urea solution (NaOH: Urea=7 wt%: 12 wt%) and stirred continuously to disperse the cellulose. After freeze-drying at -18 °C for 2 h, a clear solution with 4 wt% cellulose was obtained. A certain amount of epichlorohydrin was poured into the cellulose solution as a chemical cross-linker; the volume ratio of cross-linker to cellulose solution was 1:10. Different amounts of polyethyleneimine (0, 0.4, 0.8, and 1.2 g) were poured into the cellulose solution and mixed for 30 min, followed by ultrasonication for 15 min to remove air bubbles from the system.

The well-dispersed cellulose/crosslinker/PEI mixtures were entered into the mould and left to gel for 10 h. After gelation, the peeled hydrogels were dipped in deionized water in order to wipe off NaOH and urea from the system. The water was exchanged every 2 h until the neutral deionized water was obtained. The washed hydrogels were pre-cooled at -20 °C for 12 h and transferred for freeze-drying treatment (-50 °C, 25 Pa, 48 h).

Chemical Vapor Deposition Hydrophobic Modification

The samples were coated with methyltrimethoxysilane on the surface of cellulose through the chemical vapor deposition method. First, the cellulose/polyethyleneimine composite aerogels were put into an oven at 60 °C and set aside after 1 h. A certain amount of methyltrimethoxysilane was put into small beakers with the composite aerogels. Subsequently, the cellulose/polyethyleneimine composite aerogels were placed on the mouths and covered the mouths of the flask, in the manner of a stopper sealing the mouth of a flask. The conical flasks were placed in an oven at 105 °C for 2 h. The samples were removed and put into an oven at 70 °C for vacuum drying for 1 h, and the cellulose/ polyethyleneimine composite aerogels modified by methyltrimethoxysilane (Si-PEI-CA) were prepared.

Characterizations

The functional group changes of the cellulose aerogel were characterized by infrared spectroscopy using a Fourier Transform Infrared (FT-IR) spectrometer (Nicolet 6700, Thermo Electron, Waltham, MA, USA). The crystalline structure of the aerogel was tested by the X-ray diffraction (XRD) (D8 Advance, Bruker, Karlsruhe, Germany) with the condition of a scan rate of 5°/min in the 2θ range from 2 to 50°. A scanning electron microscope (JSM-5510LV, JEOL, Japan) was used to observe the morphology of cellulose aerogel after a gold layer was sputtered onto the fractured surface of the sample.

The quality and the volume of the cellulose aerogel were measured as a means to determine the apparent density. A true density analyzer (3H-2000 TDI, Beijing BSD Instrument, China) was used to test the true densities of the samples., and according to the Eq. 1, the apparent density and the true density of the cellulose aerogel were used to calculate the porosity (P),

$$P = 1 - \rho/\rho_s \quad (1)$$

where ρ is the apparent density of cellulose aerogel, and ρ_s is measured by true density tester.

The mechanical properties of the aerogels were tested by an electro-mechanical universal testing machine (CMT, MTS Systems Corporation), and the diameter and the height of the cylindrical test samples were 30 mm and 10 mm, respectively. The stress-

strain curve was measured at a compression speed of 1 mm/min and the compression strain of 80%. The sound absorption coefficients of the samples were carried out in an impedance tube (AWA6128A, Beijing Shi ji Jian tong Co, China).

RESULTS AND DISCUSSION

XRD tests were conducted for microcrystalline cellulose and composite aerogels. As shown in Fig. 1a, the typical diffraction peaks of microcrystalline cellulose at 16.9°, 22.9° and 34.9°, correspond to the (101), (002), and (040) crystalline faces of cellulose type I, respectively (Aym *et al*. 2019). After cellulose dissolution, the crystalline shape of the composite aerogel prepared by cross-linking changes significantly and the cellulose type I crystalline plane disappeared. The reduced peak area intensity indicated that the crystalline shape of cellulose was disrupted, and more amorphous regions and covalent bonds were formed. The results show that the cellulose went through the process of dissolution and regeneration. The crystallinity indexes (CrI) of microcrystalline cellulose and composite aerogels were calculated by the diffraction intensities of the crystalline and noncrystalline regions (Segal *et al*. 1959) (Eq. 2),

$$\mathrm{CrI}= [(I_{200}- I_{\mathrm{ma}})/ I_{200}]\times 100 \quad (2)$$

where I_{ma} is the peak intensity of noncrystalline cellulose at 18°, and I200 is the strongest peak intensity of cellulose, attributing to 200 atomic planes at 21 to 23°.

From the FTIR spectra analysis of MCC, CA and Si-PEI-CA (Fig. 1b), a broad FTIR peak of OH- stretching vibration for MCC between 3000 and 3600 cm^{-1}, because the microcrystalline celluloses contain abundant intermolecular and intramolecular hydrogen bonds. The peaks at 2970, 1343, and 1642 cm^{-1} are the C-H stretching vibration peak, C-H asymmetric bending peak, and OH- bending peak due to the absorption of water, respectively. The multiple bands from 1000 to 1200 cm^{-1} include the C-O stretching peak and COC- pyranose ring vibrations peak. The presence of two bands at 1642 cm^{-1} and a band at 1343 cm^{-1} illustrates N-H bending of acidamide and C-C bonds, respectively (Ghafari *et al*. 2019). New peaks appearing near 779 and 2970 cm^{-1} correspond to the vibrational properties of the Si-C and the Si-CH_3 bending in the Si-O-Si unit, respectively. These results imply that PEI was grafted within the cellulose aerogel and the silane bond was successfully wrapped on the surface of the short cellulose chains.

Morphological changes in the internal microstructure of different PEI/MCC samples are shown in Fig. 1(c-f). In the cross-sectional SEM images, as the PEI content increased, the microstructure exchanged from a disordered layer structure to a regular porous structure with a progressively uniform distribution of pore size. During freezing, the water slowly nucleated to produce ice crystal structures to allow the short chains of microcrystalline cellulose to concentrate into a close space. The subsequent drying process can induce the sublimated ice, creating open pore channels throughout the structure. Without PEI addition, the walls of the holes in cellulose aerogels are disrupted during the sublimation of ice crystals due to the high surface tension of water, resulting in a disordered and collapsed lamellar structure inside the pure cellulose aerogel sample. As the added PEI content increases, the pore structure of aerogel became more uniform (Fig. 1c-f). Furthermore, the corresponding porosity and skeleton density of Si-PEI-CA increased, while the apparent density decreased (Table 1), indicating that PEI can strengthen the skeleton of Si-PEI-CA and make the pore distribution of the aerogel more uniform.

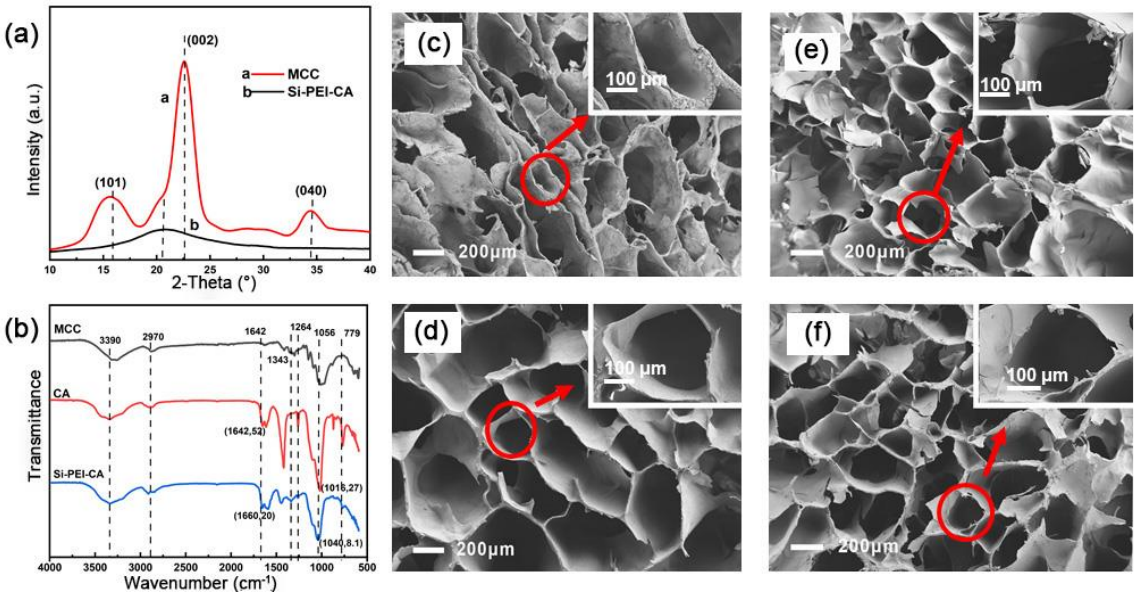

Fig. 1. (a) XRD pattern of MCC and Si-PEI-CA. (b) FTIR spectra of MCC, CA, and Si-PEI-CA. SEM images of (c) Si-0wt%PEI-CA, (d) Si-20wt%PEI-CA, (e) Si-40wt%PEI-CA, (f) Si-60wt%PEI-CA

Table 1. Apparent Density, Porosity and Skeletal Density of the Composite Aerogels at Different PEI

Sample	Apparent Density ($g•cm^{-3}$)	Porosity (%)	Skeletal Density ($g•cm^{-3}$)
Si-0 wt% PEI-CA	0.085	94.43	1.526
Si-20 wt% PEI-CA	0.081	95.22	1.679
Si-40 wt% PEI-CA	0.074	95.63	1.692
Si-60 wt% PEI-CA	0.073	95.85	1.721

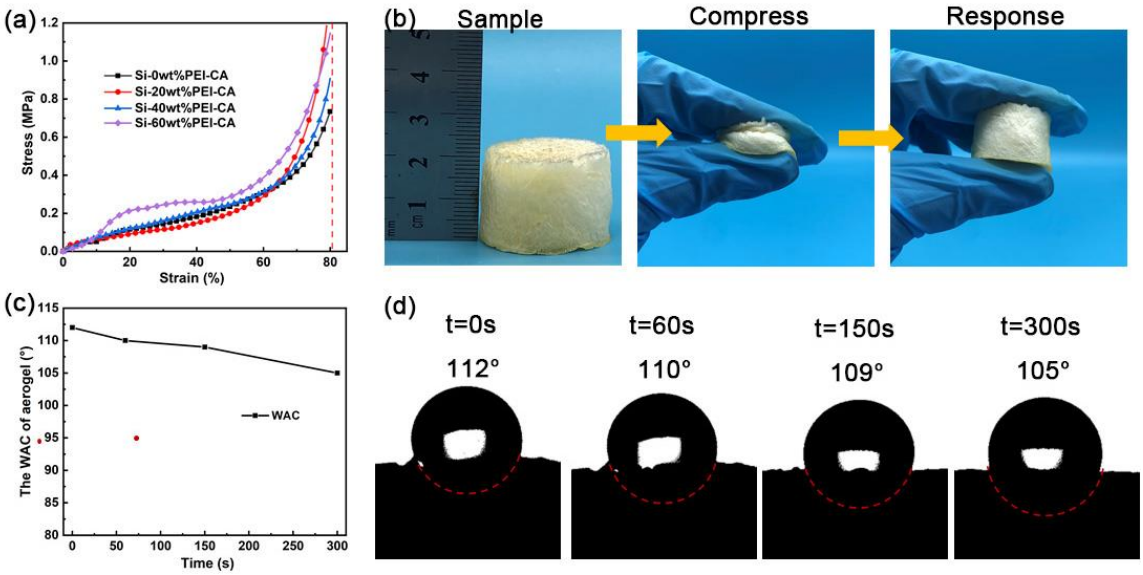

Fig. 2. (a) Stress-strain curves of Si-PEI-CA at 80% strain. (b) Compression response physical picture. (c) Trends in water contact angle. (d) Water contact angle at t=0s, t=60s, t=150s, t=300s

The stress-strain curves of the Si-PEI-CA are shown in Fig. 2. The maximum compression modulus of sample gradually increased with the increase of PEI content, and it could reach 1.1 MPa at the strain of 80% (Fig. 2a). Notably, the sample recovered quickly and naturally after compression (Fig. 2b). These results indicated that the PEI can take part in the construction of the firmer crosslinking network of the aerogels and improve the mechanical strength.

Water contact angle measurements were adopted to demonstrate the hydrophobic properties of the Si-PEI-CA. As shown in Fig. 2c, the aerogel was not significantly wetted by water, and a hydrophobic angle can be up to 112°. The water contact angle decreases slightly over time, due to the capillary penetration. These results indicate aerogel has superior hydrophobicity, which can be ascribed to the rough surface of the porous aerogel and the existence of hydrophobic -CH_3 groups on the aerogel surface.

The influences of the PEI contents and the thickness on the sound absorption property of the aerogel are illustrated in Fig. 3.

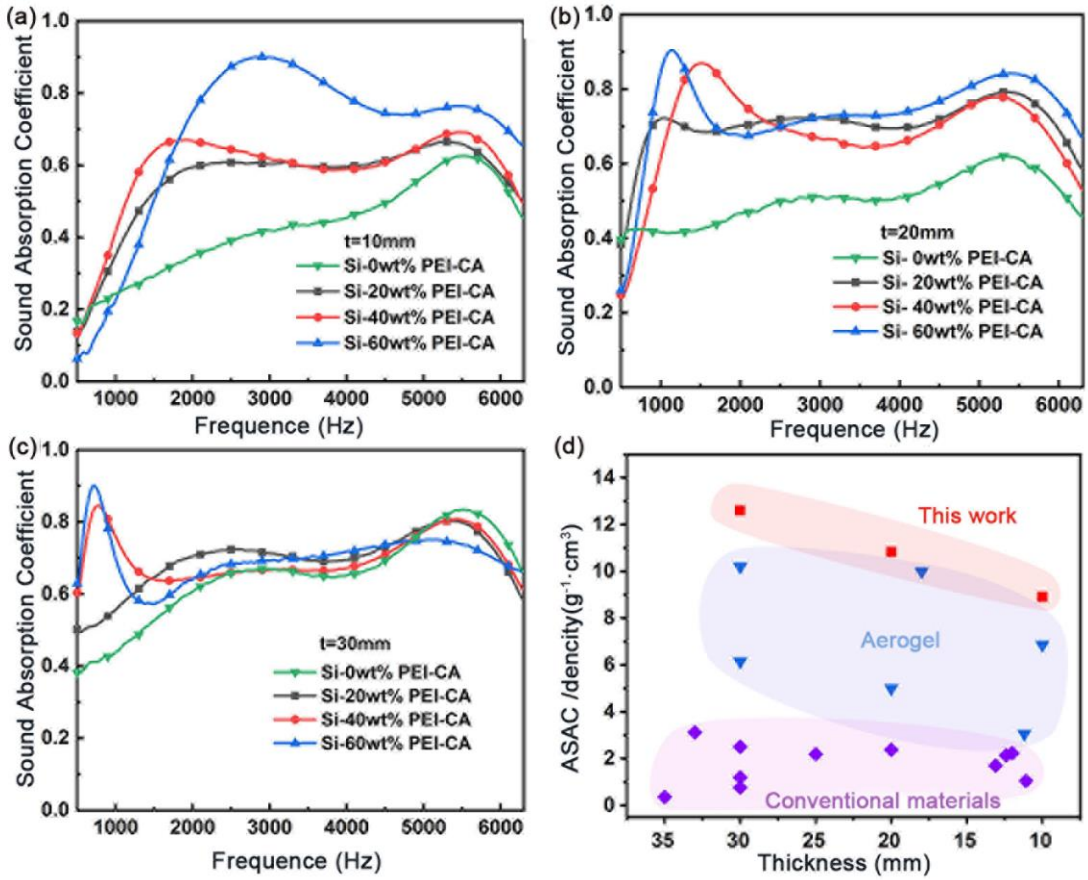

Fig. 3. Si-PEI-CA absorption coefficient at different thicknesses (a) t=10mm, (b) t=20mm, (c) t=30mm. (d) Contrast of the ASAC/density between Si-PEI-CA and previous sound absorption materials with various thicknesses

With the increase of the PEI content, the sound absorption coefficient of the cellulose aerogel improved. Due to the enhanced strength of the pore wall inside the aerogel and the more uniform distribution of the pores, it is beneficial to the reflection many times inside the material and dissipation of sound waves. Besides, increasing the thickness is beneficial to the sound absorption performance of the cellulose aerogel over a wide

frequency range, especially within a low frequency range. Satisfyingly, the average sound absorption coefficient (ASAC) exceeded 0.74 over a wide frequency range (500 to 6300 Hz) with the PEI content of 60 wt% and the thickness of 30 mm. Moreover, the ASAC/density of the Si-PEI-CA, which represents the sound absorption coefficient per unit density of the material, prevailed over the majority of the previous sound absorption materials including the traditional porous materials (Berardi and Iannace 2017; Kucukali *et al*. 2018; Wang *et al*. 2019; Taban *et al*. 2019; Yang *et al*. 2020; Li *et al*. 2021; Wang *et al*. 2021), composites (Wu and Chou 2016; Wu *et al*. 2017; Chen and Jiang 2018; Lee and Jung 2019; Liu *et al*. 2019; Pinto *et al*. 2019; Oh *et al*. 2019), and ultralight aerogels (Si *et al*. 2014; Feng *et al*. 2016; He *et al*. 2018; Cao *et al*. 2019; Jia *et al*. 2020; Shen *et al*. 2021; Pang *et al*. 2022), reflecting the obvious advantage of the Si-PEI-CA in light weight and sound absorption (Fig. 3d).

The synthetic process and mechanism of chemical cross-linking and hydrophobic modification cellulose/polyethyleneimine aerogel coated with methyltrimethoxysilane (Si-PEI-CA) are shown in Fig. 4. Cellulose is dissolved in an aqueous mixture solution of sodium hydroxide/urea solution. The long cellulose chains are broken, and the short cellulose chains are uniformly distributed in the system. The chemical reaction occurs after the addition of the crosslinker, as the epichlorohydrin opens the ring under alkaline conditions and reacts with the nucleophilic cellulose. The hydroxyl group of cellulose reacts with epichlorohydrin in a first order nucleophilic substitution reaction to form epoxidized cellulose. Owing to the reactive chemistry of ethylene oxide, the epoxide ring undergoes a nucleophilic substitution reaction following a second order reaction process. Due to the presence of a large amount of nucleophilic groups -NH_2 from PEI, a grafting reaction occurs between the epoxidized cellulose and PEI to complete cross-linking. The hydrophobic modification of the cellulose aerogel is carried out by chemical vapor deposition. Specifically, the hydrophobic modifier and the hydroxyl groups on the cellulose surface form a siloxane network, which can achieve the hydrophobic effect (Fig. 4b-c). The addition of PEI enhances the flexibility of the cellulose chains and prevents the pore structure from collapsing in the process of freeze-drying for realizing the microstructural control of the aerogels. This results in more open and semi-open pores inside the cellulose aerogel. Thereby, the hydrophobic modification with MTMS is effective obviously, preventing the pore structure from collapsing due to the absorption of water. Therefore, the high porosity, the microstructural control of the pores structure and hydrophobic modification guarantee the efficient sound absorption and widespread practical application.

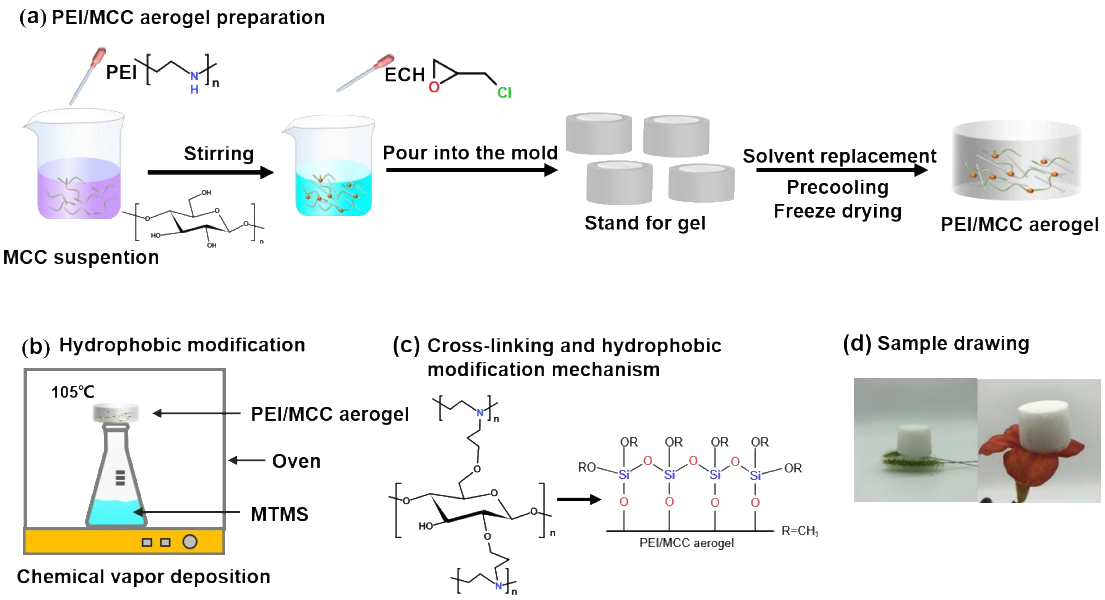

Fig. 4. Preparation process of (a) PEI/MCC aerogels, (b) hydrophobic modification. (c) chemical cross-linking and hydrophobic modification mechanism. (d) diagram of Si-PEI-CA sample

CONCLUSIONS

1. A cellulose aerogel with low apparent density, high compressibility, and hydrophobic character was prepared by a facile freeze-drying and hydrophobic process for sound absorption in a wide frequency range.
2. The effective combination of poly(ethyleneimine) (PEI) and cellulose *via* the grafting reaction and the cross-linking enhances the flexibility of the cellulose chains and prevents the pore structure from collapsing in the process of freeze-drying. This effect improved the mechanical strength, microstructural control of the aerogels, and uniform distribution of pore size.
3. The composite aerogel exhibited good hydrophobic properties with the value of WCA (112°) due to the constructed micro-nano rough layer on the surface by Si-O. The composite aerogel presents many advantages such as lightweight, high porosity, and high compression recovery.
4. The average sound absorption coefficient exceeded 0.74 over the frequency range from 500 to 6300 Hz, and the ASAC/density of the composite aerogel prevailed over the majority of the previous sound absorption materials.
5. The research demonstrated a convenient strategy to prepare environment friendly aerogels for absorbing sound waves efficiently.

ACKNOWLEDGMENTS

This work was supported by the National Natural Science Foundation of China (51273154), the Natural Science Foundation of Hubei Province (2022CFB630), the Hubei Provincial Department of Education (Q20221511) and the Graduate Innovative Fund of Wuhan Institute of Technology (CX2022217).

REFERENCES CITED

Arenas, J. P., and Crocker, M. J. (2010). "Recent trends in porous sound-absorbing materials," *Sound & Vibration* 44(7), 12-17. DOI: 10.1007/s00397-010-0453-x

Aym, A., Seb, A., and Sc, B. (2019). "Optimum alkaline treatment parameters for the extraction of cellulose and production of cellulose nanocrystals from apple pomace," *Carbohydrate Polymers* 215, 330-337. DOI: 10.1016/j.carbpol.2019.03.103

Bagheri, S., Nodoushan, R. J.. and Azimzadeh, M. (2022). "Sound absorption performance of tea waste reinforced polypropylene and nanoclay biocomposites," *Polymer Bulletin* 80(5), 5203-5218. DOI: 10.1007/s00289-022-04295-y

Berardi, U., and Iannace, G. (2017). "Predicting the sound absorption of natural materials: Best-fit inverse laws for the acoustic impedance and the propagation constant," *Applied Acoustics* 115, 131-138. DOI: 10.1016/j.apacoust.2016.08.012

Bian, H. X., Yang, Y. Y., and Tu, P. (2021). "Crystalline structure analysis of all-cellulose nanocomposite films based on corn and wheat straws," *BioResources* 16(4), 8353-8365. DOI: 10.15376/biores.16.4.8353-8365

Cao, L., Fu, Q., Yang, S., Ding, B., and Yu, J. (2018). "Porous materials for sound absorption," *Composites Communications* 10, 25-35. DOI: 10.1016/j.coco.2018.05.001

Cao, L., Si, Y., Wu, Y., Wang, X., Yu, J., and Ding, B. (2019). "Ultralight, superelastic and bendable lashing-structured nanofibrous aerogels for effective sound absorption," *Nanoscale* 11(5), 2289-2298. DOI: 10.1039/c8nr09288e

Chen, S., and Jiang, Y. (2018). "The acoustic property study of polyurethane foam with addition of bamboo leaves particles," *Polymer Composites* 39(4), 1370-1381. DOI: 10.1002/pc.24078

Cheng, F., Lu, P. B., Ren, P. F., Chen, J. B., Ou, Y. H., Lin, M. Y., and Liu, D. T. (2016). "Preparation and properties of foamed cellulose-polymer microsphere hybrid materials for sound absorption," *BioResources* 11(3), 7394-7405. DOI: 10.15376/biores.11.3.7394-7405

Duan, Y. X., Yang, H. B., Liu, K., Xu, T., Chen, J. N., Xie, H. X., Du, H. S., Dai, L., and Si, C. L. (2023). "Cellulose nanofibril aerogels reinforcing polymethyl methacrylate with high optical transparency," *Advanced Composites and Hybrid Materials* 6(3), 12. DOI: 10.1007/s42114-023-00700-w

Feng, J., Le, D., Nguyen, S. T., Nien, V. T. C., Jewell, D., and Duong, H. M. (2016). "Silica cellulose hybrid aerogels for thermal and acoustic insulation applications," *Colloids and Surfaces A: Physicochemical and Engineering Aspects* 506, 298-305. DOI: 10.1016/j.colsurfa.2016.06.052

Ghafari, R., Jonoobi, M., Amirabad, L. M., Oksman, K., and Taheri, A. R. (2019). "Fabrication and characterization of novel bilayer scaffold from nanocellulose based aerogel for skin tissue engineering applications," *International Journal of Biological*

Macromolecules 136, 796-803. DOI: 10.1016/j.ijbiomac.2019.06.104

Guo, L., Chen, Z., Lyu, S., Fu, F., and Wang, S. (2018). "Highly flexible cross-linked cellulose nanofibril sponge-like aerogels with improved mechanical property and enhanced flame retardancy," *Carbohydrate Polymers* 179, 333-340. DOI: 10.1016/j.carbpol.2017.09.084

Guo, W. W., Wang, X., Zhang, P., Liu, J. J., and Song, L. (2018). "Nano-fibrillated cellulose-hydroxyapatite based composite foams with excellent fire resistance," *Carbohydrate Polymers* 195, 71-78. DOI: 10.1016/j.carbpol.2018.04.063

He, C., Huang, J., Li, S., Meng, K., Zhang, L., Chen, Z., and Lai, Y. (2018). "Mechanically resistant and sustainable cellulose-based composite aerogels with excellent flame retardant, sound-absorption, and superantiwetting ability for advanced engineering materials," *ACS Sustainable Chemistry & Engineering* 6(1), 927-936. DOI: 10.1021/acssuschemeng.7b03281

Jia, C., Li, L., Liu, Y., Fang, B., Ding, H., Song, J., Liu, Y., Xiang, K., Lin, S., and Li, Z. (2020). "Highly compressible and anisotropic lamellar ceramic sponges with superior thermal insulation and acoustic absorption performances," *Nature Communications* 11(1), 1-13. DOI: 10.1038/s41467-020-17533-6

Kucukali Ozturk, M., Nergis, F. B., Candan, C. (2018). "Design of electrospun polyacrylonitrile nanofiber–coated nonwoven structure for sound absorption," *Polymers for Advanced Technologies* 29(4), 1255-1260. DOI: 10.1002/pat.4236

Lee, J., and Jung, I. (2019). "Tuning sound absorbing properties of open cell polyurethane foam by impregnating graphene oxide," *Applied Acoustics* 151, 10-21. DOI: 10.1016/j.apacoust.2019.02.029

Li, B., Xu, W. Y., Kronlund, D., Maattanen, A., Liu, J., Smatt, J. H., Peltonen, J., Willfor, S., Mu, X. D., and Xu, C. L. (2015). "Cellulose nanocrystals prepared via formic acid hydrolysis followed by tempo-mediated oxidation," *Carbohydrate Polymers* 133, 605-612. DOI: 10.1016/j.carbpol.2015.07.033

Li, X., Yu, X., and Zhai, W. (2021). "Additively manufactured deformation-recoverable and broadband sound-absorbing microlattice inspired by the concept of traditional perforated panels," *Advanced Materials* 33(44), article 2104552. DOI: 10.1002/adma.202104552

Lim, Z. Y., Putra, A., Nor, M. J. M., and Yaakob, M. Y. (2018). "Sound absorption performance of natural kenaf fibres," *Applied Acoustics* 130, 107-114. DOI: 10.1016/j.apacoust.2017.09.012

Liu, L., Chen, Y. J., Liu, H. Z., Rehman, H. U., Chen, C., Kang, H. M., and Li, H. (2019). "A graphene oxide and functionalized carbon nanotube based semi-open cellular network for sound absorption," *Soft Matter* 15(10), 2269-2276. DOI: 10.1039/c8sm01326h

Lu, Y., Sun, Q., Yang, D., She, X., Yao, X., Zhu, G., Liu, Y., Zhao, H., and Li, J. (2012). "Fabrication of mesoporous lignocellulose aerogels from wood via cyclic liquid nitrogen freezing–thawing in ionic liquid solution," *Journal of Materials Chemistry* 22(27), 13548-13557. DOI: 10.1039/c2jm31310c

Moroe, N., and Mabaso, P. (2022). "Quantifying traffic noise pollution levels: A cross-sectional survey in South Africa," *Scientific Reports* 12(1), 11. DOI: 10.1038/s41598-022-07145-z

Oh, J. H., Lee, H. R., Umrao, S., Kang, Y. J., and Oh, I. K. (2019). "Self-aligned and hierarchically porous graphene-polyurethane foams for acoustic wave absorption," *Carbon* 147, 510-518. DOI: 10.1016/j.carbon.2019.03.025

Pang, K., Liu, X., Pang, J., Samy, A., Xie, J., Liu, Y., Peng, L., Xu, Z., and Gao, C. (2022). "Highly efficient cellular acoustic absorber of graphene ultrathin drums," *Advanced Materials* e2103740. DOI: 10.1002/adma.202103740

Park, S. H., Lee, M., Seo, P. N., Kang, E. C., and Kang, C. W. (2020). "Acoustical properties of wood fiberboards prepared with different densities and resin contents," *BioResources* 15(3), 5291-5304. DOI: 10.15376/biores.15.3.5291-5304

Pedroso, M., De Brito, J., and Silvestre, J. D. (2017). "Characterization of eco-efficient acoustic insulation materials (traditional and innovative)," *Construction and Building Materials* 140, 221-228. DOI: 10.1016/j.conbuildmat.2017.02.132

Pinto, S. C., Marques, P. A. A. P., Vesenjak, M., Vicente, R., Godinho, L., Krstulovic-Opara, L., and Duarte, I. (2019). "Mechanical, thermal, and acoustic properties of aluminum foams impregnated with epoxy/graphene oxide nanocomposites," *Metals* 9(11), 1214. DOI: 10.3390/met9111214

Rafieian, F., Hosseini, M., Jonoobi, M., and Yu, Q. (2018). "Development of hydrophobic nanocellulose-based aerogel via chemical vapor deposition for oil separation for water treatment," *Cellulose* 25(8), 4695-4710. DOI: 10.1007/s10570-018-1867-3

Ren, S. W., Zou, W. R., Sun, W., Zhang, T. Y., Zhang, J. Y., Zeng, X. Y. and Xu, Y. (2022). "Manufacturing and semi-analytical modeling of environment-friendly sound absorbent porous glasses," *Applied Acoustics* 185, 9. DOI: 10.1016/j.apacoust.2021.108444

Salino, R. E., and Catai, R. E. (2023). "A study of polyurethane waste composite (PUR) and recycled plasterboard sheet cores with polyurethane foam for acoustic absorption," *Construction and Building Materials* 387, 11. DOI: 10.1016/j.conbuildmat.2023.131201

Samaei, S. E., Berardi, U., Mahabadi, H. A., Soltani, P., and Taban, E. (2023). "Optimization and modeling of the sound absorption behavior of polyurethane composite foams reinforced with kenaf fiber," *Applied Acoustics* 202, 12. DOI: 10.1016/j.apacoust.2022.109176

Segal, L., Creely, J. J., Martin, J. A. E., and Conrado, C.M. (1959). "An empirical method for estimating the degree of crystallinity of native cellulose using the X-ray diffractometer," *Textile Research Journal* 29(10), 786-794. DOI: 10.1177/004051755902901003

Shen, L., Zhang, H., Lei, Y., Chen, Y., Liang, M., and Zou, H. (2021). "Hierarchical pore structure based on cellulose nanofiber/melamine composite foam with enhanced sound absorption performance," *Carbohydrate Polymers* 255, article 117405. DOI: 10.1016/j.carbpol.2020.117405

Si, Y., Yu, J., Tang, X., Ge, J., and Ding, B. (2014). "Ultralight nanofibre-assembled cellular aerogels with superelasticity and multifunctionality," *Nature Communications* 5(1), 5802. DOI: 10.1038/ncomms6802

Soatthiyanon, N., Aumnate, C., and Srikulkit, K. (2020). "Rheological, tensile, and thermal properties of poly(butylene succinate) composites filled with two types of cellulose (kenaf cellulose fiber and commercial cellulose)," *Polymer Composites* 41(7), 2777-2791. DOI: 10.1002/pc.25575

Taban, E., Tajpoor, A., Faridan, M., Samaei, S. E., and Beheshti, M. H. (2019). "Acoustic absorption characterization and prediction of natural coir fibers," *Acoustics Australia* 47(1), 67-77. DOI: 10.1007/s40857-019-00151-8

Wan, C., Jiao, Y., and Li, J. (2016). "Influence of pre-gelation temperature on mechanical properties of cellulose aerogels based on a green NaOH/PEG solution—A comparative study," *Colloid and Polymer Science* 294(8), 1281-1287. DOI: 10.1007/s00396-016-3887-6

Wang, J. Q., Du, B., and Huang, Y. (2022). "Experimental study on airborne sound insulation performance of lightweight double leaf panels," *Applied Acoustics* 197, 9. DOI: 10.1016/j.apacoust.2022.108907

Wang, J. Z., Ao, Q. B., Ma, J., Kang, X. T., Wu, C., Tang, H. P., and Song, W. D. (2019). "Sound absorption performance of porous metal fiber materials with different structures," *Applied Acoustics* 145, 431-438. DOI: 10.1016/j.apacoust.2018.10.014

Wang, Y., Guo, J., Fang, Y., Zhang, X., and Yu, H. (2021). "Ultralight metamaterial for sound absorption based on miura-ori tessellation structures," *Advanced Engineering Materials* 23(12), article 2100563. DOI: 10.1002/adem.202100563

Wang, Z., Liu, S., Matsumoto, Y., and Kuga, S. (2012). "Cellulose gel and aerogel from LiCl/DMSO solution," *Cellulose* 19(2), 393-399. DOI: 10.1007/s10570-012-9651-2

Wu, C. M., and Chou, M. H. (2016). "Sound absorption of electrospun polyvinylidene fluoride/graphene membranes," *European Polymer Journal* 82, 35-45. DOI: 10.1016/j.eurpolymj.2016.07.001

Wu, Y., Sun, X. Y., Wu, W., Liu, X., Lin, X. Y., Shen, X., Wang, Z. Y., Li, R. K. Y., Yang, Z. Y., Lau, K. T., and Kim, J. K. (2017). "Graphene foam/carbon nanotube/poly(dimethyl siloxane) composites as excellent sound absorber," *Composites Part A – Applied Science and Manufacturing* 102, 391-399. DOI: 10.1016/j.compositesa.2017.09.001

Yang, J., Han, C. R., Zhang, X. M., Xu, F., and Sun, R. C. (2012). "Cellulose nanocrystals mechanical reinforcement in composite hydrogels with multiple cross-links: Correlations between dissipation properties and deformation mechanisms," *Macromolecules* 47(12), 4077-4086. DOI: 10.1021/ma500729q

Yang, T., Hu, L. Z., Xiong, X. M., Petru, M., Noman, M. T., Mishra, R., and Militky, J. (2020). "Sound absorption properties of natural fibers: A review," *Sustainability* 12(20), article 8477. DOI: 10.3390/su12208477

Zhang, T., Zhang, Y., Wang, X., Liu, S., and Yao, Y. (2018). "Characterization of the nano-cellulose aerogel from mixing CNF and CNC with different ratio," *Materials Letters* 229, 103-106. DOI: 10.1016/j.matlet.2018.06.101

Zhou, X., Fu, Q., Liu, H., Gu, H., and Guo, Z. (2020). "Solvent-free nanoalumina loaded nanocellulose aerogel for efficient oil and organic solvent adsorption," *Journal of Colloid and Interface Science* 581, 299-306. DOI: 10.1016/j.jcis.2020.07.099

Article submitted: August 17, 2023; Peer review completed: September 9, 2023; Revised version received and accepted: September 20, 2023; Published: October 26, 2023.
DOI: 10.15376/biores.18.4.8432-8443